International Journal of Wavelets, Multiresolution
and Information Processing
Vol. 6, No. 6 (2008) 777–798

BANDWIDTH EMPIRICAL MODE DECOMPOSITION AND ITS APPLICATION

QIWEI XIE[*,†], BO XUAN[‡], SILONG PENG[‡], JIANPING LI[†,§]
WEIXUAN XU[†] and HUA HAN[‡],

[*]*School of Management*
University of Science and Technology of China
Hefei, 230026, P. R. China

[†]*Institute of Policy and Management*
Chinese Academy of Sciences
Beijing, 100080, P. R. China

[‡]*Institute of Automation*
Chinese Academy of Sciences
Beijing, 100080, P. R. China
[§]*ljp@casipm.ac.cn*

Received 1 August 2007
Revised 20 January 2008

There are some methods to decompose a signal into different components such as: Fourier decomposition and wavelet decomposition. But they have limitations in some aspects. Recently, there is a new signal decomposition algorithm called the Empirical Mode Decomposition (EMD) Algorithm which provides a powerful tool for adaptive multi-scale analysis of nonstationary signals. Recent works have demonstrated that EMD has remarkable effect in time series decomposition, but EMD also has several problems such as scale mixture and convergence property. This paper proposes two key points to design Bandwidth EMD to improve on the empirical mode decomposition algorithm. By analyzing the simulated and actual signals, it is confirmed that the Intrinsic Mode Functions (IMFs) obtained by the bandwidth criterion can approach the real components and reflect the intrinsic information of the analyzed signal. In this paper, we use Bandwidth EMD to decompose electricity consumption data into cycles and trend which help us recognize the structure rule of the electricity consumption series.

Keywords: Intrinsic Mode Function (IMF); Empirical Mode Decomposition (EMD); sifting algorithm; instantaneous frequency.

AMS Subject Classification: 15A90, 65Y99

[§]Corresponding author.

1. Introduction

There are several methods to decompose a time series into different cycles and trends. One of the most fundamental methods is the Fourier decomposition, which deem the signals as a linear combination of harmonic components. Although the Fourier transform is valid under extremely general conditions, there are some crucial restrictions of the Fourier spectral analysis: the system must be linear and the data must be strictly periodic or stationary. In recent years, wavelet decomposition has been developing rapidly. But if the mother wavelet is selected, we will have to use it to analyze all the data. Except non-adaptive nature, the problem of the most commonly used wavelet is its leakage generated by the limited of the basic wavelet function, which makes the quantitative definition of the energy-frequency-time distribution difficult.

Empirical mode decomposition, introduced by Huang *et al.*,[1,2] is a method for decomposing complex, multi-component signal into several elementary Intrinsic Mode Functions (IMFs). Differing from Fourier and wavelet analysis which have predefined basis, EMD uses only scale and frequency characters of the original signal. EMD is a local, fully data-driven and self-adaptive analysis approach. Moreover, the combination of the EMD method and the associated Hilbert spectral analysis can offer a powerful method for time frequency analysis.

Although it often proved remarkable effect in many applications, such as engineering mechanics,[3] image processing[4,10] and signal processing,[6,9] EMD method has several drawbacks. Firstly, it lacks a mathematical base which can represent EMD method naturally. Secondly, it is a pity that the criteria,[1,7,8,11] considered so far are all constraints on the amplitude and have nothing to do with the frequency or phase of the IMF so that IMF obtained based on those criteria will have dramatically different frequencies and cause scale mixing problem. The paper improved EMD algorithm based on the two aspects and used updated EMD algorithm to analysis a time sequence about electricity consumption.

In the next section, we introduce the Empirical Mode Algorithm. In the third section, we provide convergent property of EMD and present an example which leads to stop criterion problem. The fourth section contains stop criterion overview of the SD criterion, 3-thresholds criterion, EDT criterion, Damerval criterion and a detailed Bandwidth Stop criterion which includes bandwidth definition, instantaneous frequency estimation and our sifting algorithm. Finally, Bandwidth EMD is used to decompose a simulated series and one electricity consumption series. We analyze the results carefully and compare the results with other criterion. The sixth section concludes the paper.

2. EMD Basics

In order to let its instantaneous frequency (IF) have a meaningful interpretation, the IMF has to satisfy two conditions: (1) in the whole data set, the number of extrema and the number of zero-crossings must either equal or differ at most by one; (2) at any point, the local average of upper and lower envelop is zero. The EMD uses sifting process to extract IMF form the analyzed signal. The sifting process actually serves two purposes: to eliminate riding waves and to smooth uneven amplitudes. The following presents the EMD method in brief. The details with regard to the implementation of the EMD algorithm are available in Ref. 1.

2.1. *Sifting process*

Given a real valued signal $x(t)$, let $r(t) = x(t)$, $k = 1$, $i = 0$, the process of EMD can be summarized as follows

(1) Find all local minima and maxima of $r(t)$.
(2) Get the upper envelop $e_{\max}(t)$ by interpolating between maxima. Similarly get the lower envelop $e_{\min}(t)$ with minima.
(3) Compute the mean envelop as an approximation to the local average, $m(t) = (e_{\max}(t) + e_{\min}(t))/2$.
(4) Let $i = i + 1$ and define the proto-mode function (PMF) as $p_i(t) = r(t) - m(t)$, and let $r(t) = p_i(t)$.
(5) Repeat Steps 1–4 on PMF $p_i(t)$ until it is an IMF, then record the IMF $imf_k(t) = p_i(t)$.
(6) Let $r(t) = r(t) - imf_k(t)$, if the extremum point number of $r(t)$ is larger than three, let $k = k+1$, $i = 0$, and go to Step 1; otherwise, finish the sifting process.

3. Convergent Property

EMD deems that the extreme point has reflected the frequency essence information and separates different frequency components step by step according to the position and value of extreme point. In order to comprehend EMD better, we need to consider the convergence property. But we consider convergence property of EMD based on the phenomenon that the number and position of extreme points are approximately invariable when sifting process iterates excessively. In order to exhibit the algorithm conveniently, we give three definition and one assumption.

Definition 3.1. Given time-series S, matrix A_u is called upper envelop matrix if the following property hold: A_uS is upper envelop of time series S.

Definition 3.2. Given time-series S, matrix A_l is called lower envelop matrix if the following property hold: A_lS is lower envelop of time series S.

Definition 3.3. Given time-series S, matrix A is called envelop matrix if the following property hold: AS is mean envelop of time series S.

Hypothesis 1. The position of extreme point is invariable when sifting process iterates sufficiently.

Under the definition and assumption, the EMD sifting procedure is rewritten as follows:

(1) Set $S_0 = S = x$, given a threshold τ and $i = 1$.
(2) Find the local extremal points.
(3) Construct a matrix A_{i-1} that computes the mean value of the upper and lower envelops.
(4) Compute $S_i = S_{i-1} - A_{i-1}S_{i-1}$.
(5) If is $\|A_{i-1}S_i\|$ smaller than a given threshold, terminate the algorithm; otherwise, go to Step 2.

Theorem 3.1. *Eigenvalue of upper envelope A_u is either* 0 *or* 1*.*

Proof. The signal S length is N. Set local maxima point sequence $\{x_{m_i}\}$, $i \in \Delta$, Δ is index of the local maxima sequence and the total number is L. We denote $\Omega = [m_1, \ldots, m_L] \subset [1, \ldots, N]$. Actually A_u is written as $A_u = BC$ (C a matrix meaning the maxima position can be presented as $R^{L\times N}$. B is interpolation coefficient matrix which can be presented as $R^{N\times L}$).

$$C(m,n) = \begin{cases} 1 & \text{if } S(m_i) \geq S(m_i - 1) \text{ and } S(m_i) \leq S(m_i + 1), \\ 0 & \text{else.} \end{cases} \tag{3.1}$$

In our proof, we take the cubic spline interpolation as the interpolation of the EMD algorithm. The 0th non-uniform B-spline function, is defined as follows

$$N_{m_i,0}(m,n) = \begin{cases} 1 & \text{if } m_j \leq x \leq m_{j+1}, \\ 0 & \text{otherwise.} \end{cases} \tag{3.2}$$

From De Boor,[5] the recursion formula is given by

$$\begin{aligned} N_{m_j,k} &= \omega_{m_j,k} N_{m_j,k-1} + (1 - \omega_{m_{j+1},k}) N_{m_{j+1},k-1}, \\ \omega_{m_j,k} &= \frac{x - m_j}{m_{j+k} - m_j} \quad \text{for } k > 0. \end{aligned} \tag{3.3}$$

A sequence $\{c^2_{m_j}(k), m_j \in \Delta, k \in \Delta\}$, is solved by

$$\sum_{k=1}^{L} c^2_{m_j} N_{m_k,4}(x)|_{x=m_j} = \delta_{m_j,0}. \tag{3.4}$$

So we can define

$$L_{j,4} = \sum_{k=1}^{L} c^2_{m_j}(k) N_{m_k,4}(x). \tag{3.5}$$

And then, we have $B(:,i) = [L_{i,4}(1), \ldots, L_{i,4}(N)]^T$, where $[\cdot]^T$ denote transpose. From Eq. (3.4), it is trivial to get that

$$\begin{cases} B(m_i, i) = 1, \\ B(m_{j,j\neq i}, i) = 0, \\ B(k,i) = L_{i,4}(k) \quad \text{if } k \,\bar{\in}\, \Omega. \end{cases} \tag{3.6}$$

From $A_u = BC$, we get

$$\begin{cases} A(:,k) = [0, \ldots, 0, \ldots, 0] \quad \text{if } k \,\bar{\in}\, \Omega, \\ A(:,m_i) = B(:,i). \end{cases} \tag{3.7}$$

From Eqs. (3.6) and (3.7), we know the structure of matrix A_u and B. The proof of the theorem will be completed if we can find the eigenvector and eigenvalue of A_u. Primarily, we consider a group vectors $\{e_j^T = (0,\ldots,0,\underset{j}{1},0,\ldots,0), j \,\bar{\in}\, \Omega\}$. It is easy to obtain $A_u(k,:)e_j = 0$, because $A_u(k,m) = 0$, if $m \,\bar{\in}\, \Omega, 1 \leq k \leq N$. For another group vectors $\{X_i, X_i = B(:,i), i \in \Omega\}$, it follows that

$$\begin{aligned} A_u(k,:)X_i &= \sum_{j\in\Omega, j\neq i} A_u(k,j)X_i(j) + \sum_{j \,\bar{\in}\, \Omega} A_u(k,j)X_i(j) + A_u(k,i)X_i(i) \\ &= \sum_{j\in\Omega, j\neq i} A_u(k,j)B(j,i) + \sum_{j \,\bar{\in}\, \Omega} 0 \cdot X_i(j) + A_u(k,i) \cdot 1 \\ &= A_u(k,i) \\ &= X_i(k). \end{aligned}$$

Therefore, it verifies that spectral radius of upper envelop matrix is either 0 or 1. Furthermore, $\{e_j^T = (0,\ldots,0,\underset{j}{1},0,\ldots,0), j \,\bar{\in}\, \Omega\}$ and $\{X_i, X_i = B(:,i), i \in \Omega\}$ are eigenvectors, which is corresponding to eigvenvalue 0 and 1. □

Theorem 3.2. *Spectral radius of lower envelop matrix A_d is either* 0 *or* 1*.*

Proof. This follow immediately from Theorem 3.1. □

Theorem 3.3. *Spectral radius of a matrix that computes the mean value A of the upper and lower envelops is between* 0 *and* 1*.*

Proof. The conclusion is easy from the Theorems 3.1 and 3.2. □

Theorem 3.4. *The EMD sifting algorithm converges under the Hypothesis* 1 *condition.*

Proof. If we want to prove the convergence of the EMD algorithm, in fact we need to prove the convergence of the sequence S_i. For the sake of obtaining S_i

convergence property, we turn to discussing the convergence of $U_i = S - S_i$. We define $U_i = 0$, when $i = 0$. Hence from the definition of U_i, it follows that

$$U_i = S - S_1 + S_1 - S_2 + \cdots + S_{i-1} - S_i. \tag{3.8}$$

We can simplify $S_{i-1} - S_i$ to the expression

$$S_{i-1} - S_i = S_i - (S_{i-1} - AS_i) = AS_{i-1}. \tag{3.9}$$

From the EMD sifting procedure Step 4 which is rewritten by us, we get

$$AS_{i-1} = A(I - A)S_{i-2} = \cdots = A(I - A)^{i-1}S. \tag{3.10}$$

From Eqs. (3.8)–(3.10), we obtain

$$U_i = \sum_{k=0}^{i-1} A(I - A)^k, \quad \text{when } i \geq 1. \tag{3.11}$$

If we suppose that $\lambda_1, \lambda_2, \ldots, \lambda_m$ are eigenvalues of A, $1 - \lambda_1, 1 - \lambda_2, \ldots, 1 - \lambda_m$ are eigenvalues of $1 - A$. And so $\lambda_1(1 - \lambda_1)^k, \lambda_2(2 - \lambda_2)^k, \ldots, \lambda_m(1 - \lambda_m)^k$ are eigenvalues of $A(I - A)^k$. From Theorem 3.3, it obtains $0 \leq \lambda_i \leq 1$. If there exists $\lambda_i = 1$, it implies $\lambda_i(1 - \lambda_i)^k = 0$. It follows that $0 < \lambda_i(1 - \lambda_i)^k < 1$ for $\lambda_i \neq 1, 0$. Therefore, we obtain

$$\gamma(A(I - A)^k) = \max(\lambda_1(1 - \lambda_1)^k, \lambda_2(1 - \lambda_2)^k, \ldots, \lambda_m(1 - \lambda_m)^k) < 1,$$

where $\gamma(\cdot)$ represtens spectral radius.

It is easily perceived that $\sum_{k=0}^{p-1} z(1 - z)^k$ is convergent, when $0 \leq z \leq 1$. Based on the matrix theory, we conclude that $\sum_{k=0}^{i-1} A(I - A)^k$ is convergent. So U_i has been proved to be convergent, we conclude that EMD sifting algorithm is convergent under Hypothesis 1. □

Through our proof, it can be seen that if sifting iteration steps are enough, the algorithm is convergence and gets the corresponding IMF. It seemed that the algorithm ought to iterate more and even iterate unlimited as much as that we can get the IMFs which reflect the time series essential nature. But it is not consistent with the reality, we introduce the following example.

Example 1.

$$x_1 = 4\sin(20\pi t)\sin(\pi t),$$

$$x_2 = \sin(10\pi t),$$

$$x_3 = x_1 + x_2.$$

Sampling interval is 0.01, which is shown in Fig. 1.

From Example 1, it can be concluded that the result does not reflect the nature when iteration number is too much. If iteration number is too much, the sifting algorithm reduces the amplitude variety extensively. So the decomposition results

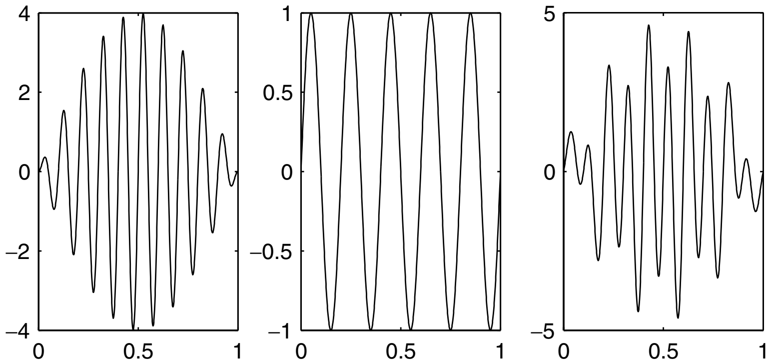

Fig. 1. Time-series x_1, x_2, x_3.

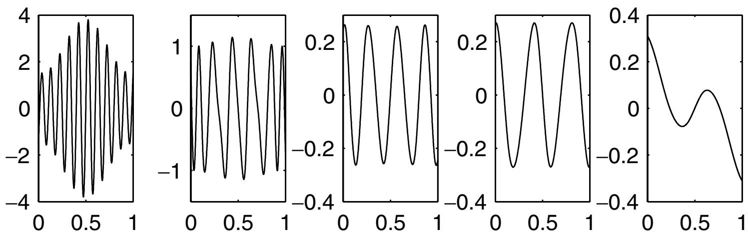

Fig. 2. Result of sifting process whose iteration steps are attained 5000.

lack fidelity. Then how to choose stop criterion that makes the sifting iteration procedure stop appropriately? We will design the stop criterion and our stop criterion next chapter.

4. Stop Criterion Improvement

4.1. *IMF stop criterion*

The second condition for IMF is too rigid to use, so we need improve it in the implementation of EMD. The essential of the improvement is to make the instantaneous frequency of IMF meaningful. To guarantee the IMF components retain enough physical sense, Huang[1] limit the size of the standard deviation, SD can be obtained by the two consecutive PMFs as follows

$$\mathrm{SD} = \sum_t \frac{|p_{k-1}(t) - p_k(t)|^2}{p_{k-1}^2(t)}. \tag{4.1}$$

The SD is a Cauchy-type criterion. Since the SD is unrelated to the definition of IMF, the component obtained by this criterion could not be an IMF.

As an improvement to the SD criterion, Rilling[11] brought forward a 3-threshold criterion. Let the 3-thresholds are θ_1, θ_2 and α. Then let $a(t) = (e_{\max} - e_{\min})/2$ and $\sigma(t) = |m(t)/a(t)|$. Sifting process is iterated until t, $\sigma(t) < \theta_1$ for fraction $(1-\alpha)$ of the total time and for the remaining fraction. The typically value of the thresholds are: $\alpha \approx 0.05$, $\theta_1 \approx 0.05$ and $\theta_2 \approx 0.5$. Furthermore, in the same paper, a local EMD criterion was proposed to overcome the contaminating problem caused by singular area of total time. The shortcoming of the 3-thresholds criterion is that the thresholds do not adapt to the signal.

Recently, Cheng[8] put forward the energy difference tracking method based on the assumption that the residue and IMFs are orthogonal mutually. Suppose the signal shown in (4.2) contains a finite number of mutually orthogonal components $x_i(t), i = 1, 2, \ldots, N$, and the average of $x_i(t)$ is zero. Then we have

$$\int x_i(t)x_j(t) \approx 0, \quad i \neq j. \tag{4.2}$$

When EMD decomposes and obtains an IMF $c_1(t)$, and after $c_1(t)$ has been separated from $x(t)$, the energy variation caused by decomposition is

$$E_{err} = \left| \int c_1^2(t)dt - \int x(t)c_1(t)dt \right|. \tag{4.3}$$

Then the smaller the E_{err}, the more entire integrity and orthogonal the IMFs will be. Hence, we can track E_{err} when the signal is decomposed by EMD method. When E_{err} reaches a certain minimum and the mean value of envelops becomes small enough, sifting process is completed and then comes to the next IMF's iteration. Thus the obtained IMF component is an orthogonal one of the original signal. However, the EDT criterion cannot select the correct PMF as IMF when real components of the analyzed signal have strong correlations. The energy difference tracking method is based on the assumption that the IMFs are orthogonal. However, the IMFs of nonlinear and nonstationary signals are not orthogonal. Even for linear and stationary signals, the real components of the discrete signal we get will not be orthogonal because of environment noise and sampling. For these reasons, the energy difference tracking method cannot guarantee that the IMF is the best approximation of the real component.

Damerval[7] proposed a criterion based on the number of iterations and the number of IMFs for bidimensional EMD. This criterion saves computational cost and has little boundary effect in sifting process. The number of iterations and IMFs should be selected carefully. Too few sifting steps cannot eliminate the riding waves and the obtained IMFs will dissatisfy the two IMF conditions. On the other hand, too many sifting steps would sometimes obliterate the intrinsic amplitude variations and make the results physically less meaningful.

Additionally, none of the before-mentioned criteria uses the frequency or phase information of the analyzed signal. So IMFs obtained with those criteria are prone to have scale mixing problem, and then have no reasonable interpretation.

Xuan and Xie[16,17] designed a new stop criterion-bandwidth criterion. And we will discuss the new stop criterion next subsection.

4.2. *Bandwidth stop criterion*

Given a real valued signal $x(t)$, using the analytic signal theory can get a complex valued signal whose real part equals to $x(t)$. So we use complex signal directly. Given a signal $z(t) = a(t)\exp(j\varphi(t))$, the instantaneous frequency of $z(t)$ is $d\varphi/dt$. A signal has meaning in instantaneous frequency if and only if it is a monocomponent signal the sum of two unequal strength tones. For lack of exact definition of the monocomponent signal was given by now, Huang,[1] used the two IMF condition to replace monocomponent. The paper put forward local narrow band signal to substitute monocomponent. A signal $z(t) = a(t)\exp(j\varphi(t))$ is narrowband if and only if $a(t)$ is a band-limited signal and the highest frequency of $a(t)$ is far less than $d\varphi/dt$. If any little component of a signal is narrow band, the signal is called a local narrowband signal. The IMF conditions can get good component from the analyzed signal sometimes, but the instantaneous frequencies of IMFs are usually are meaningless because the IMFs are not monocomponent. Consider a signal which is composed of N AM-FM component signals

$$z(t) = a(t)\exp(j\varphi(t)) = \sum_{m=1}^{N} a_m(t)\exp(j\varphi_m(t)) \tag{4.4}$$

where $a_m(t)$, $\varphi_m(t)$ are the amplitude and phase function, respectively. Then

$$a^2 = \sum_{m=1}^{N} \omega_m(t), \tag{4.5}$$

$$\omega_m(t) = \sum_{n=1}^{N} a_m a_n \cos(\varphi_m(t) - \varphi_n(t)). \tag{4.6}$$

We can get

$$\frac{d\varphi}{dt} = \sum_{m=1}^{N} \frac{w_m(t)}{a^2(t)} \frac{d\varphi_m}{dt} + \frac{1}{a^2(t)} \sum_{m=1}^{N} \sum_{n=1}^{N} \frac{da_m}{dt} a_n(t)\sin(\varphi_m(t) - \varphi_n(t)). \tag{4.7}$$

If we have established the followed two conditions

$$\omega_m(t) \geq 0, \tag{4.8}$$

$$\sum_{m=1}^{N} \sum_{n=1}^{N} \frac{da_m}{dt} a_n(t)\sin(\varphi_m(t) - \varphi_n(t)) = 0\,, \tag{4.9}$$

we can guarantee that $d\varphi/dt$ is interpreted as a nonnegative weighted average of the instantaneous frequency and instantaneous frequency stays within the instantaneous spectral range of $x(t)$ at time t. But Eqs. (4.8) and (4.9) defined the conditions are too strict, we modified some changes in Eqs. (4.10) and (4.11)

$$D_\varphi(t) = \sup_{1\le m\le N}\left|\frac{d\varphi}{dt} - \frac{d\varphi_n}{dt}\right| \tag{4.10}$$

$$D_\varphi(t) \ge \frac{\max\limits_{1\le m\le N}\left(\frac{d\varphi_m}{dt}\right) - \min\limits_{1\le n\le N}\left(\frac{d\varphi_n}{dt}\right)}{2}. \tag{4.11}$$

So the smaller $D_\varphi(t)$, the instantaneous frequency at time t will be more significant. On the other hand, the instantaneous bandwidth[14,15] of the signal at time t is

$$B_t = \sigma_{\omega|t} = |a'/a|. \tag{4.12}$$

So when B_t is very small, $z(t)$ is construed as a local narrowband signal. Moreover, the smaller B_t is, the smaller $|d\varphi_m/dt - d\varphi_n/dt|$. And then from (4.11), the smaller $|d\varphi_m/dt - d\varphi_n/dt|$, the larger probability of $D_\varphi(t)$ has small value. So the instantaneous frequency has perfect physical sense only when B_t is very small, the details of instantaneous frequency is available in Refs. 9 and 10. From the knowledge of Fourier analysis, $S(\omega)$ is Fourier transform of $z(t)$, and B is the bandwidth of $z(t)$, then we can get

$$B^2 = \sigma_\omega^2 = \int_{-\infty}^{\infty}(\omega - \langle\omega\rangle)^2|S(\omega)|^2 d\omega = \int_{-\infty}^{\infty} z(\bar{t})\left(\frac{1}{j}\frac{d}{dt} - \langle\omega\rangle\right)^2 z(t)dt. \tag{4.13}$$

Substitute $z(t) = a(t)\exp(j\varphi(t))$ into (4.13) then obtain

$$B^2 = B_a^2 + B_f^2, \tag{4.14}$$

where

$$B_a^2 = \int_{-\infty}^{\infty}\left(\frac{a'}{a}\right)^2 a^2(t)dt, \tag{4.15}$$

$$B_f^2 = \int_{-\infty}^{\infty}\left(\frac{d\varphi}{dt}\right)^2 a^2(t)dt. \tag{4.16}$$

Equation (4.14) implies that B^2 is the sum of two terms. B_a^2 results from the change of amplitude $a(t)$ and only associates with amplitude modulating. Furthermore, B_a^2 is the nonnegative weighted sum of instantaneous bandwidth. We call B_f^2 as frequency bandwidth. B_f^2 results from the change of instantaneous frequency $\varphi'(t)$ and reflects the consistency of instantaneous frequency at all time extended. The smaller B_f^2, the closer the scale characters at different time, and the milder the scale mixing problem. So we can take B_f^2 as a stop criterion.

4.3. *Instantaneous frequency estimation*

There are many algorithms to compute instantaneous frequency, such as phase differencing of the analytic signal, Teager–Kaiser operator, counting the zero-crossings, and adaptive estimation methods based on the Least Mean Square (LMS) algorithm, etc. Since IF should be unrelated with amplitude, we choose zero-crossings points to estimate the frequency of the analytic signal. For a sinusoidal signal, the frequency is given by the inverse of the period, or alternatively by half the inverse of the interval between zero-crossings, i.e.

$$f = \frac{1}{2T_z} \tag{4.17}$$

or

$$f = \frac{1}{2}, \tag{4.18}$$

where T_z is the interval between zero crossings, $2T_z$ is the period, f is the frequency, and Z is the zero-crossing rate. To reduce the variance of the zero-crossings estimate, an estimator is defined by

$$f(n) = \frac{z(n)}{2} \tag{4.19}$$

$$Z(n) = \sum_{m=-M}^{M} |\text{sgn}(s(m)) - \text{sgn}(s(m-1))| h(n-m) \tag{4.20}$$

where M is a window length,

$$\text{sgn}(s(n)) = \begin{cases} 1 & \text{for } s(n) \neq 0, \\ -1 & \text{for } s(n) < 0, \end{cases}$$

$$h(n) = \begin{cases} \dfrac{1}{2M} & \text{for } 0 \leq n \leq M, \\ 0 & \text{otherwise.} \end{cases}$$

The details are available in Ref. 15. The variance of f is defined by σ_f^2. The smaller the σ_f^2, the closer the frequencies at different sample points are. If we get a minimum for σ_f^2 during sifting process, we consider that current signal is an IMF.

4.4. *Our sifting algorithm*

Given a real valued signal $x(t)$, let $r(t) = x(t)$, $k = 1$, $i = 0$, the process of EMD can be summarized as follows:

(1) Find all local minima and maxima of $r(t)$.
(2) Get the upper envelop $e_{\max}(t)$ by interpolating between maxima. Similarly, get the lower envelop $e_{\min}(t)$ with minima.
(3) Compute the mean envelop as an approximation to the local average, $m(t) = (e_{\max}(t) + e_{\min}(t))/2$.

(4) Let $i = i + 1$ and extract the proto-mode function (PMF) $p_i(t) = r(t) - m(t)$, and let $r(t) = p_i(t)$.

(5) Repeat Steps 1–4 on PMF, stop criterion is presented by next three subsidiary processes:

  (5.1) Use 3-thresholds $(\alpha_1, \theta_1, \theta_2)$ criterion to get PMF that almost satisfies the two conditions of IMF.

  (5.2) Continue the sifting process until we find the minimum of σ^2_{PMF} or until the difference of σ^2_{PMF} between two consequent PMF is very small, which is estimator from Chap. 4.3.

  (5.3) Take the final PMF as an IMF, then the IMF has small frequency bandwidth mild scale mixing problem. Then record the IMF $imf_k(t) = p_i(t)$.

(6) Let $r(t) = r(t) - imf_k(t)$, if the extremum point number of $r(t)$ is larger than T, let $k = k + 1$, $i = 0$, and go to Step 1; otherwise finish the sifting process.

5. Simulated Experiment and Economic Data Analysis

5.1. *Simulated experiment*

The follows illustrate the decomposition results obtained with 3-threshold, EDT, Damerval criterion and bandwidth criterion, respectively. In order to compare EDT and bandwidth criterion, we choose a signal whose components are almost orthogonal mutually.

As shown in (5.1) and Fig. 3, the simulated signal $x(t)$ consists of an amplitude modulated signal and a sine signal

$$\begin{aligned} x_1 &= 4\sin(20\pi t)\sin(0.2\pi t), \\ x_2 &= \sin(10\pi t), \\ x_3 &= x_1 + x_2, \end{aligned} \tag{5.1}$$

where $t \in [0, 1]$, and sampling frequency is 1024 Hz.

The thresholds used in this paper are: $\alpha = 0.05$, $\theta_1 = 0.05$ and $\theta_2 = 0.5$ for 3-thresholds and energy difference tracking criterion; $\alpha = 0.1$, $\theta_1 = 0.5$ and $\theta_2 = 0.5$ for bandwidth criterion; the number of iterations is 100 for Damerval criterion.

Suppose the IMF corresponding to $x_i(t)$ is $c_i(t)$, we define the error signal between $x_i(t)$ and $c_i(t)$

$$D_i(t) = |x_i(t) - c_i(t)| \tag{5.2}$$

and define

$$E_{dif}(i) = \sqrt{\int D_i^2(t)dt} \tag{5.3}$$

where $D(t)$ describes the performance of EMD. $E_{dif}(i)$ is the distance between $x_i(t)$ and the corresponding IMF.

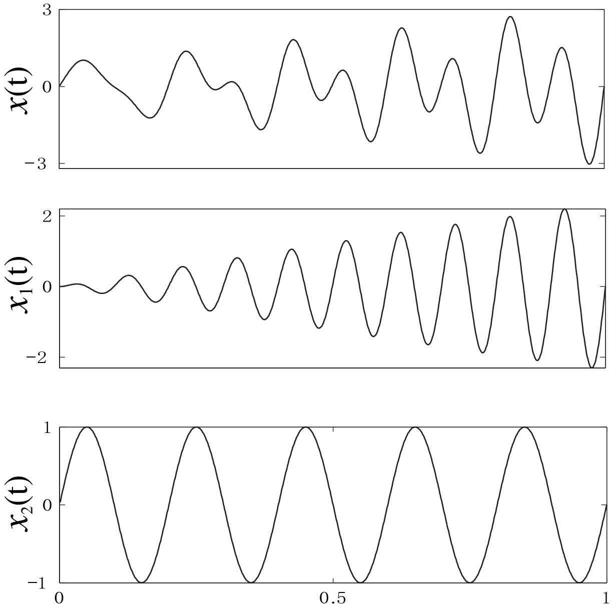

Fig. 3. The simulated signal and its two components.

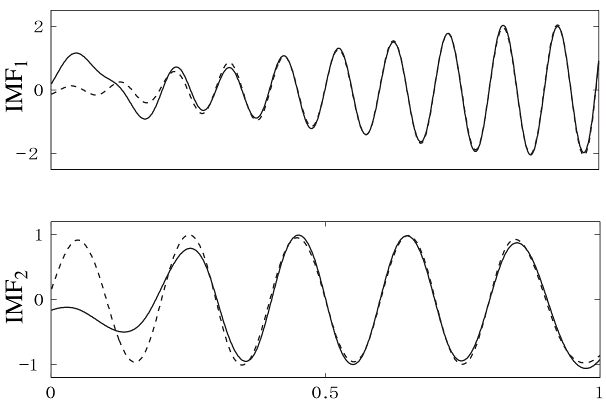

Fig. 4. IMFs of $x(t)$ obtain with 3-threshold criterion (real lines) and bandwidth criterion (lash lines).

Figure 2 presents the decomposition results of $x(t)$ with 3-threshold criterion and bandwidth criterion. It is clearly illustrated that the foresides of IMFs obtained with 3-threshold criterion are all anamorphic and lose their physical sense. As shown in Fig. 3, the IMFs obtained with 3-threshold and Damerval criterion have scale mixing problem because spectrum lines are disordered near 5 Hz. On the contrary, the IMFs obtained with bandwidth have slight scale mixing problem and are close to the real components. From Fig. 4, we know that $D(t)$ with bandwidth criterion

Table 1. E_{dif} of the simulated signal with different IMF criterion.

Criterion	3-Threshold	Damerval Criterion	Energy Difference Tracking	Bandwidth
$E_{dif}(1)$	0.331	0.198	0.110	0.107
$E_{dif}(2)$	0.254	0.161	0.110	0.105

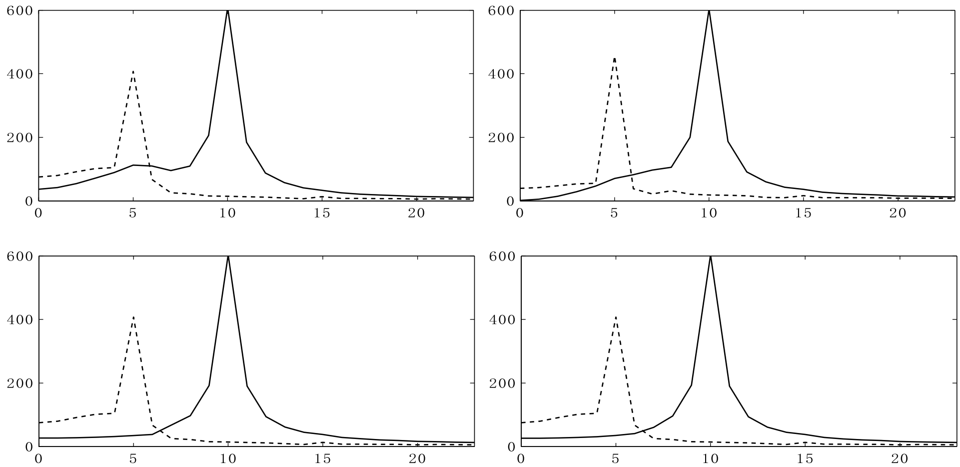

Fig. 5. The Fourier spectrums for the IMFs of $x(t)$ with different sift criteria. Real lines are spectrum for IMF1, and lashed lines are spectrum for IMF2. From top to bottom and left to right: criterion is 3-threshold, Damerval, energy difference tracking and bandwidth.

are smaller than $D(t)$ with the other three criteria in the majority of this time range. Table 1 illustrates that the bandwidth criterion gets the best approximations to the real components of $x(t)$. In addition, $c_2(t)$ needs only one iteration with bandwidth criterion. This confirms that the numbers of sifting iterations are adaptive to signal automatically.

This example also shows that the bandwidth criterion has some superiority over the EDT criterion even when the real components are nearly orthogonal mutually. The details are available in Ref. 16.

5.2. *Economic data analysis*

Poland everyday electricity consumption[18,19] from 1990 to 1994 is used to evaluate the performance of our proposed algorithm. This time-series is shown in Fig. 7.

Business and economic time series frequently exhibit seasonality-period fluctuations that recur with about the same intensity each year. Economists[20–22] are far more interested in the delicate patterns of the fluctuations which are superimposed upon the trend only in order to see these patterns more clearly. From prior knowledge, we know that electricity consumption is related with climate and human activity. We might conclude that the time-series can be decomposed as

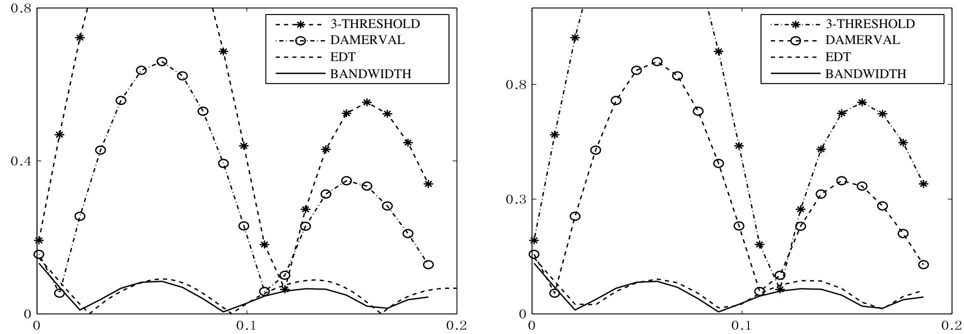

Fig. 6. Part of $D(t)$ with difference criteria. Left: $D_1(t)$. Right: $D_2(t)$.

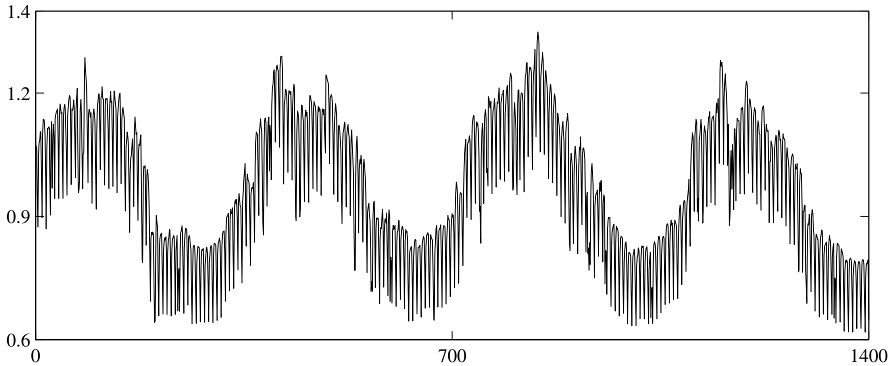

Fig. 7. The electricity load values of Poland from 1990's.

some components which are corresponding with the four seasons or human activity cycles. Let's review the decomposition result and contrasting outcome using other decomposition methods.

If we cannot use the bandwidth stop criterion, we will get the result which is not perfect. So we will show the compared result in Figs. 9–12. Figures 9–11 are not used bandwidth stop criterion and Fig. 12 is used. The left part of the figures is Hilbert spectrum of the IMF which is the seasonal component corresponding to the cyclic part that the period is one year. The thresholds that are used in the paper are $\alpha_1 = 0.01$, $\theta_1 = 0.01$ and $\theta_2 = 0.1$ for 3-threshold of all the stop criterion; and the number of iterations is 10 for Damerval criterion. From the Fig. 9, we see that band criterion reflects more essential content and the result confirms seasonal factor. It is shown that our sifting process can improve the result which is shown in Fig. 8. We will analyze the electricity consumption using result from our proposed algorithm and obtain some periodic rules of the electricity consumption.

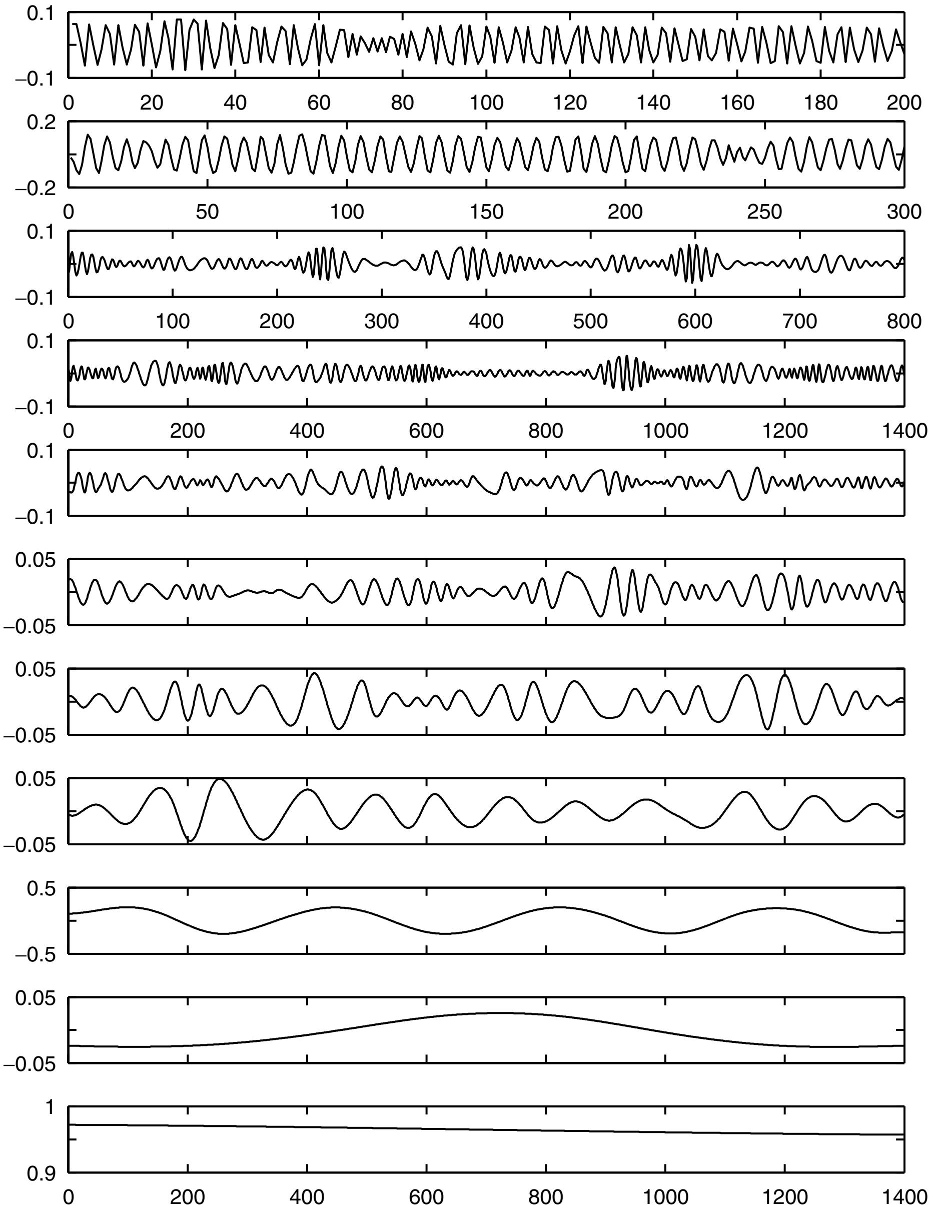

Fig. 8. Result of our sifting process.

We set up the time-series as $x(t)$ which is shown by Fig. 7. The decomposition result is $imf_i(t)$, $i = 1, \ldots, 11$, and $imf_{11}(t)$ is the trend item. Define the energy and energy ratio to investigate the decomposition items

$$E(f) = \int |f(t)|^2, \quad \text{thereupon } \mathrm{E}(imf_{\mathrm{i}}) = \sum_{\mathrm{t}=1}^{1400} imf_{\mathrm{i}}^2(\mathrm{t}), \tag{5.4}$$

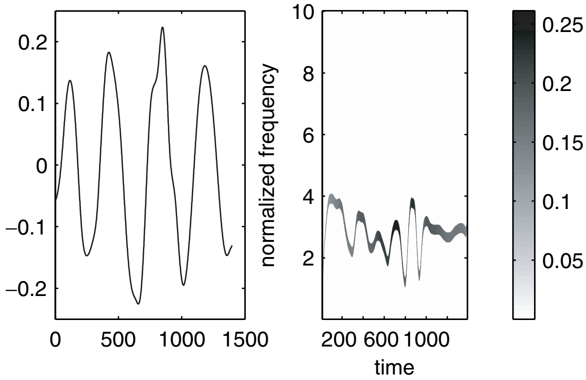

Fig. 9. The 8th IMF with 3-threshold criterion[4] and its Hilbert spectrum.

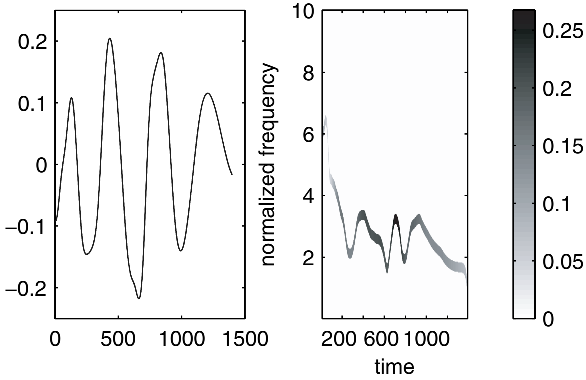

Fig. 10. The 6th IMF of Damerval criterion and its Hilbert spectrum.

$$Er_i = \frac{\sqrt{E_i}}{\sum_{i=1}^{10} \sqrt{E_i}}. \tag{5.5}$$

We use the energy as defined in (5.4) and energy ration as defined in (5.5) to sieve the IMFs in order to delete some IMFs rooted from scale mixture. Computational result and its comparison shown in Table 2 are obviously items $imf_1(t)$, $imf_2(t)$, $imf_9(t)$ and the trend item. Other items are mixture items which are leaked from the actually items. $imf_1(t)$, $imf_2(t)$, $imf_9(t)$ and $imf_{11}(t)$ can reconstruct the $f(t)$. Further investigate the function

$$f_1(t) = imf_1(t) + imf_2(t) + imf_9(t) + imf_{11}(t). \tag{5.6}$$

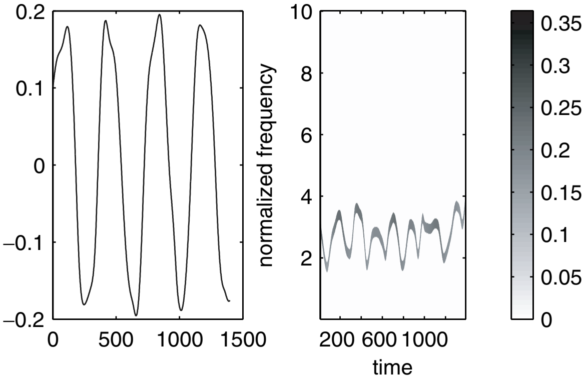

Fig. 11. The 9th IMF of energy criterion and its Hilbert spectrum.

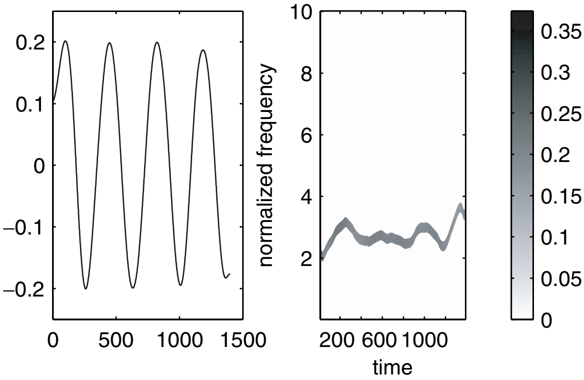

Fig. 12. The 9th IMF of bandwidth criterion and its Hilbert spectrum.

The difference between reconstructed functions f_1 and f is measured by the absolute error ratio and the similarity ratio, respectively, which are presented by

$$\sqrt{\frac{E(f-f_1)}{E(f)}} = 0.0483 \quad \text{(absolute error ratio)},$$

$$\frac{\sum(f-\bar{f})(f_1-\bar{f}_1)}{\sqrt{E(f-\bar{f})E(f_1-\bar{f}_1)}} = 0.9587 \quad \text{(similarity ratio)},$$

where $\bar{f}$ is mean of f. Similarity ratio measure the correlation between the two functions. The reconstructed function f_1 approximate f according to above two standards, which is shown in Fig. 13.

Firstly, we analyze the trend item $imf_{11}(t)$. Figure 8 shows the trend item $imf_{11}(t)$ that is obviously a slow-moving descendent trend. But if it is not decomposed the time-series we cannot get the trend.

Table 2. The decomposition results.

IMFs	Energy	E_r	IMFs	Energy	E_r
imf_1	2.6086	0.1127	imf_6	0.2403	0.0342
imf_2	7.3184	0.1888	imf_7	0.4998	0.0493
imf_3	0.5162	0.0502	imf_8	0.5107	0.0499
imf_4	0.4027	0.0443	imf_9	28.2983	0.3713
imf_5	0.4662	0.0477	imf_{10}	0.5446	0.0515

Table 3. The position of extrema and zero-crossings of imf_9.

Extrema	183	348	540	727	921	1091	1280
Z-Cs	99	260	448	632	823	1008	1186

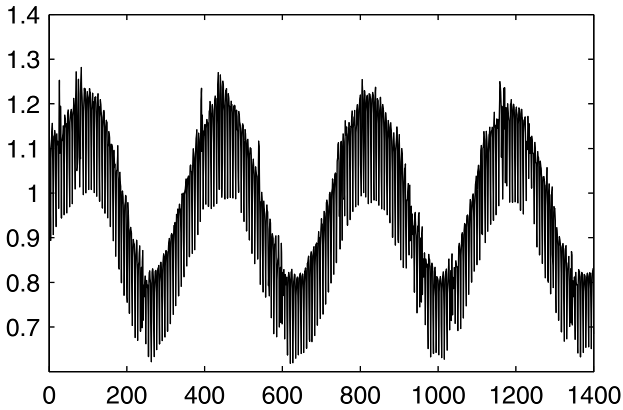

Fig. 13. Reconstructed time series.

The item $imf_9(t)$ is local-narrowed function. We investigate the zero-crossings and extreme points from Table 3. I and II denote zero-crossings, extreme points respectively. The interval of zero-crossings is 182.8 and the interval of extreme points is 180.85. If we consider the interval of zero-crossings and extreme points, we gain the result that $imf_9(t)$ is regarded as a year periodic time-series.

For $imf_2(t)$, is high-frequency component, extreme points population is very large. We count the interval extreme points' distribution to express the periodicity. The interval distribution of the maximal points is shown by right component of Fig. 14. So it can be concluded that $imf_2(t)$ is a week periodic series.

Similarly, the interval distribution of $imf_1(t)$ is shown by the left component of Fig. 14 and we conclude that $imf_1(t)$ is half-week periodic series. From Fig. 7, we gain that the electricity consumption presents the periodic rules, but these rules are mixed and contained noise. If we apply our sifting algorithm, we can separate

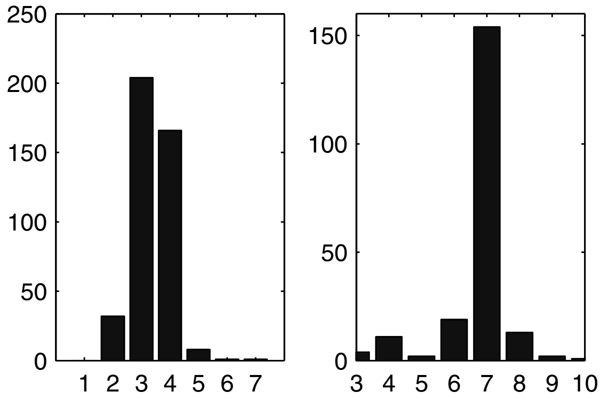

Fig. 14. The periodic distribution of $imf_1(t)$ and $imf_2(t)$.

the periodic rules. So we obtain three key conclusions:

I The consumption of electricity is slowly descended from 1990 to 1994 which appears from the trend item imf_{11};

II The consumption of electricity expresses periodic property which is, respectively half-week, one week and one year;

III These three kinds of motions of period is obviously stronger than any other motions, so we should pay attention to these motions of period when we are confronted with electricity coordination.

This kind of periodic analysis is helpful to assign national electricity power. We can gain from the result and be able to decide when to carry on maintaining it, when we should allow a full burden of equipments revolve and at which particular time we should pay attention to.

6. Conclusions

The results of this study are based on EMD algorithm. EMD algorithm is a succinct and valid technique for some engineering application, but the EMD algorithm has two problems: scale mixture and convergence property. We design a new stop criterion-bandwidth criterion which cannot only find the IMFs reflecting the scale and frequency characters of the analyzed time series but also make the IMFs have reasonable meaning. Except that IMFs obtained with bandwidth criterion have slighter scale mixing effect.

The performance of the EMD algorithm is presented in many fields, but it is almost not some application on the economic domain with EMD algorithm. So we use the Bandwidth EMD algorithm to analyze the electricity consumption data, where the decomposition components corresponding to the climate or man activity orderliness are easily selected. From all the sifting above, although we have not used any prior information and have selected a fixed basic function, we find the components have reflected the nature character of the time series. So the results prove that the Bandwidth EMD is a potential tool for applied economics.

Acknowledgments

This research is supported by the National Natural Science Foundation of China under Grant No. 70531040 and CASIA Innovation Fund for Young Scientists.

References

1. N. E. Huang *et al.*, The empirical mode decomposition and the Hilbert spectrum for nonlinear and non-stationary time series analysis, *Proc. Roy. Soc. Lond. Ser. A.* **454** (1998) 903–995.
2. N. E. Huang, Z. Shen and S. R. Long, A new view of nonlinear water waves: The Hilbert Spectrum, *Ann. Rev. Fluid Mech.* **31** (1999) 417–457.
3. Y. L. Xu, M. Asce and J. Chen, Structural damage detection using empirical mode decomposition: Experimental investigation, *J. Eng. Mech.* **130(11)** (2004) 1279–1288.
4. Z. Liu and S. Peng, Boundary processing of bidimensional EMD using texture synthesis, *IEEE Signal Process. Lett.* **12** (2005) 33–36.
5. C. De Boor, *A Practical Guide to Splines* (Springer-Verlag, 2001).
6. P. Flandrin, G. Rilling and P. Goncalves, Empirical mode decomposition as a filter bank, *IEEE Signal Process. Lett.* **11**(2) (2004) 112–114.
7. C. Damerval, S. Meignen and V. Perrier, A fast algorithm for bidimensional EMD, *IEEE Signal Process. Lett.* **12**(10) (2005) 123–125.
8. J. S. Cheng *et al.*, Research on the intrinsic mode function (IMF) criterion in EMD method, *Mech. Syst. Signal Process.* **20** (2006) 817–824.
9. H. G. Li and G. Meng, Detection of harmonic signals from chaotic interference by empirical mode decomposition, *Chaos Solitons Fractals* **30**(4) (2006) 930–935.
10. B. Shen, Estimating the instantaneous frequencies of a multicomponent AM-FM image by bidimensional empirical mode decomposition, in *Proc. IEEE Int. Workshop on Intelligent Signal Processing* (WISP'05), Faro, Portugal (2005), pp. 283–287.
11. G. Rilling, P. Flandrin and P. Goncalves, On empirical mode decomposition and its algorithms, in *Proc. IEEE-EURASIP Workshop on Nonlinear Signal and Image Processing* (NSIP'03), Grado, Italy (2003), 5 pp; http://perso.ens-lyon.fr/paulo.goncalves/pub/emd-eurasip03.pdf.
12. P. Loughlin and B. Tacer, Comments on the interpretation of instantaneous frequency, *IEEE Signal Process. Lett.* **4** (1997) 123–125.
13. D. Wei and A. C. Bovik, On the Instantaneous frequencies of multicomponent AM-FM signals, *IEEE Signal Process. Lett.* **45** (1997) 867–869.
14. L. Cohen, *Time-Frequency Analysis* (Prentice-Hall, NJ, 1995).
15. B. Boashash, Estimating and interpreting the instantaneous frequency of a signal, *Proc. IEEE.* **80(4)** (1992) 519–569.
16. B. Xuan, Q. Xie and S. Peng, EMD sifting based on bandwidth, *IEEE Signal Process. Lett.* **14**(8) (2007) 537–540.
17. Q. Xie and B. Xuan, EMD algorithm based on bandwidth and the application on one economic data analysis, in *Proc. European Signal Processing Conference*, Poznań, Poland (2007), pp. 2419–2423.
18. G. Simon, A. Lendasse and M. Cottrell, Time series forecasting: Obtaining long term trends with self-organizing maps, *Pattern Recogn. Lett.* **26** (2005) 1795–1808.

19. A. Lendasse, P. Cardon and V. Wertz, Forecasting electricity consumption using non-linear projection and self-organizing maps, *Neurocomputing* **48** (2002) 299–311.
20. M. Baxter and R. G. King, Measuring business cycles: Approximate band-pass filters for economic time series, *Rev. Econ. Stat.* **81**(4) (1999) 575–593.
21. A. C. Harvey and T. Trimbur, General model-based filters for extracting cycles and trends in economic time series, *Rev. Econ. Stat.* **85**(2) (2003) 244–255.
22. D. S. G. Pollock, Methodology for trend estimation, *Econ. Mod.* **18**(1) (2001) 75–96.